Numerical Analysis of Three Section Distributed Bragg Reflector Tunable Laser Diode with Modified Oscillation Condition Based on the Transfer Matrix Method

M. H. Yavari[1], *V. Ahmadi[1, 2], F. Shahshahani[3], M. Razaghi[1]
[1]Dept. of Elect. Eng., Tarbiat Modares University, Tehran, Iran
[2]Laser Research Center, AEOI, Tehran, Iran
[3]Dept. of Physics, Al-Zahra University, Tehran, Iran

Abstract- **We present a detailed analysis of the static tuning characteristics of three-section tunable DBR laser using transfer matrix method. The key feature of the analysis is the use of modified oscillation condition. With exact oscillation condition, the static tuning characteristics such as threshold current, output power, oscillating wavelength are obtained and the effects of a discontinuity at the active- passive interface and also the manufacturing imperfections on the device characteristics are investigated.**

I. INTRODUCTION

Tunable lasers are very attractive for a variety of applications in future communications, such as dense WDM, local oscillator tuning in coherent optical communication systems, and optical switching in local area networks [1-4]. Several works have been done on the theory of wavelength tuning in multielectrode DBR lasers [5-11]. The previous works on the three-section DBR device by Pan *et al*. [6], Patzak *et al*. [7] Caponio *et al*. [8] have been extended by Tsigopoulos *et al*. [9] however the effect of active-passive interface in oscillation condition is not considered. This paper describes a detailed model with modified oscillation condition which considers the effect of discontinuity and misalignment at active-passive interface. The paper organized as follows: In section II the theory of the model is presented. The results are discussed in section III and finally, conclusion is brought in section IV.

II. THE MODEL

A schematic diagram of a three-section DBR laser is shown in Fig. 1. It consists of three longitudinally integrated waveguide sections: an active Fabry-Perot section providing the optical gain for the laser operation, a passive phase control (PC) section which contains neither gratings nor active material and a passive DBR mirror section. The three sections have separate electrodes and are assumed electrically isolated from each other. By injecting current into one of the passive sections, the carrier density increases which leads to a decrease of the refractive index due to the free-carrier plasma effect and a subsequent increase of the Bragg frequency.

A. Modification of Oscillation Condition

The analysis is based on the transfer matrix method (TMM) [12-16], transmission line [17-18] and scattering theory [15].

* Corresponding Author
Dept. of Elect. Eng., Tarbiat Modares University
P.O. BOX 14115-143, Tehran, Iran.
E-mail: v_ahmadi@modares.ac.ir

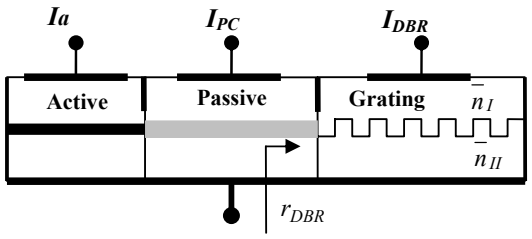

Fig. 1. Schematic diagram of three section tunable DBR laser

By considering the active-passive interface, and using transmission line theory, we obtain the modified oscillation condition for the lasing modes:

$$\frac{(S_{11}S_{22}-S_{12}S_{21})\cdot r_{DBR}e^{-j2\tilde{\beta}_2 L_2}-S_{11}}{S_{22}r_{DBR}e^{-j2\tilde{\beta}_2 L_2}-1}\cdot r_1\cdot e^{-j2\tilde{\beta}_1 L_1}=1 \quad (1)$$

where L_1 and L_2 are the length of active and passive section respectively. r_{DBR} is the effective reflectivity of the DBR section including the reflectivity at the right facet and r_1 is the facet reflectivity at the left end of the structure. S_{11}, S_{22}, S_{12} and S_{21} are the elements of scattering matrix at the interface between active-passive section [9].

$$S_{11}=\frac{\bar{n}_1-\bar{n}_2}{\bar{n}_1+\bar{n}_2}+R \quad (2)$$

$$S_{22}=\frac{\bar{n}_2-\bar{n}_1}{\bar{n}_1+\bar{n}_2}-R' \quad (3)$$

$$S_{21}=\frac{\sqrt{2R(\bar{n}_1+\bar{n}_2)(\bar{n}_2-\bar{n}_1)-R^2(\bar{n}_1+\bar{n}_2)^2-|C_L|^2(\bar{n}_1+\bar{n}_2)^2+4\bar{n}_1\bar{n}_2}}{(\bar{n}_1+\bar{n}_2)} \quad (4)$$

S_{12} is given by expression (4) if one replaces R by R'. $\bar{n}_1$ and $\bar{n}_2$ are the refractive index of active and passive sections, respectively. $|C_L|^2$ expresses the amount of energy lost at interface. R and R' represent the additional reflection due to the waveguide misalignment at the active-passive interface and are also input parameters to the model.

The complex wave numbers for the three sections are given by

$$\tilde{\beta}_1(\omega,N_1)=\frac{\omega}{c}\bar{n}_1(\omega,N_1)+\frac{j}{2}[\Gamma_1 g_1(\omega,N_1)-\alpha_1(N_1)] \quad (5)$$

$$\tilde{\beta}_i(\omega, N_i) = \frac{\omega}{c}\bar{n}_i(\omega, N_i) - \frac{j}{2}\alpha_i(N_1), \quad \text{(i=2,3)} \qquad (6)$$
$$= \frac{\omega}{c}[\bar{n}_0 + \Delta\bar{n}_i(N_i)] - \frac{j}{2}[\alpha_0 + \Delta\alpha_i(N_i)]$$

c is the light velocity in vacuum, Γ_1 is the confinement factor of the active section, ω is the angular optical frequency; N_1, N_2, and N_3 are the carrier densities in the active, the phase and the DBR sections. $\bar{n}_1$ and α_1 are the effective refractive index and internal absorption of the active section, $\bar{n}_2$ and $\bar{n}_3$ are the effective refractive indexes of the phase and DBR sections. ω is the frequency of oscillation, $g_1(\omega, N_1)$ is the modal gain of the active section, and $\bar{n}_0$ and α_0 are the effective refractive index and internal absorption of the passive sections in the absence of carrier injection. The carrier-induced index and absorption changes are expressed as [6], [9], [17].

$$\Delta\bar{n}_i(N_i) = \Gamma\frac{dn}{dN}N_i \qquad (7)$$

$$\Delta\alpha_i(N_i) = \Gamma\frac{d\alpha}{dN}N_i \qquad (8)$$

where Γ is the confinement factor, and dn/dN and $d\alpha/dN$ are material parameters. The characteristic equation (1) is separated in its real and imaginary parts:

$$-\xi\cdot r_1|r_{DBR}|\exp(2\alpha_{th}L_1 - \alpha_2 L_2) \cdot\sin\left[2\left(\frac{\omega\bar{n}_1 L_1}{c} + \frac{\omega\bar{n}_2 L_2}{c} - \frac{\varphi}{2}\right)\right] \qquad (9)$$
$$= -S_{11}r_{ap}r_1\exp(2\alpha_{th}L_1)\sin(2\frac{\omega\bar{n}_2 L_2}{c}) + S_{22}\cdot|r_{DBR}|\exp(-\alpha_2 L_2)\sin\left[2\left(\frac{\omega\bar{n}_2 L_2}{c} - \frac{\varphi}{2}\right)\right]$$

$$1+\xi\cdot r_1|r_{DBR}|\exp(2\alpha_{th}L_1 - \alpha_2 L_2) \cdot\cos\left[2\left(\frac{\omega\bar{n}_1 L_1}{c} + \frac{\omega\bar{n}_2 L_2}{c} - \frac{\varphi}{2}\right)\right] \qquad (10)$$
$$= S_{11}\cdot r_1\exp(2\alpha_{th}L_1)\cos(2\frac{\omega\bar{n}_2 L_2}{c}) + S_{22}\cdot|r_{DBR}|\exp(-\alpha_2 L_2)\cos\left[2\left(\frac{\omega\bar{n}_2 L_2}{c} - \frac{\varphi}{2}\right)\right]$$

where $r_{ap} = (\bar{n}_1 - \bar{n}_2)/(\bar{n}_1 + \bar{n}_2)$, $r_{DBR} = |r_{DBR}|\exp(j\varphi)$ $\xi = S_{11}S_{22} - S_{12}S_{21}$, $\alpha_{th} = (\Gamma_1 g_1(\omega, N_1) - \alpha_1(N_1))/2$. In the case when $C_L = 0$, $R = 0$, $R' = 0$ then $\xi = -1$, $S_{22} = -r_{ap}$, $S_{11} = r_{ap}$ and the above equations concide with the oscillation conditions given by Tsigopoulos *et al* [9] and when $\bar{n}_1 = \bar{n}_2$ and the effect of misalignment is neglected, the above equation leads to the oscillation conditions given by Pan et al [6]. When $\bar{n}_1 \neq \bar{n}_2$, $C_L \neq 0$, $R \neq 0$ and $R' \neq 0$ the equations presented in [6] and [9] give only an approximation of (9) and (10). In general case, one has to solve simultaneously the complex relations (9) and (10) numerically, with respect to ω and α_{th} in order to find the oscillation conditions $(\omega^m, \alpha_{th}^m)$ of the m_{th} mode.

B. Bragg Grating Section Model

The Bragg grating section can be modeled by interpreting grating structures with transfer matrix [12]. The transfer matrix for one corrugation period in the Bragg grating section is obtained from the matrices of a homogeneous waveguide and refractive index step.

$$T = \frac{1}{t}\begin{bmatrix}1 & r\\ r & 1\end{bmatrix}\begin{bmatrix}e^{j\tilde{\beta}_{II}l} & 0\\ 0 & e^{-j\tilde{\beta}_{II}l}\end{bmatrix}\frac{1}{t}\begin{bmatrix}1 & -r\\ -r & 1\end{bmatrix}\begin{bmatrix}e^{j\tilde{\beta}_{I}l} & 0\\ 0 & e^{-j\tilde{\beta}_{I}l}\end{bmatrix} \qquad (11)$$

$$r = \frac{\bar{n}_I - \bar{n}_{II}}{\bar{n}_I + \bar{n}_{II}}, \quad t = \sqrt{1-r^2} \qquad (12)$$

where $\tilde{\beta}_I = \omega\bar{n}_I/c - j\alpha_3/2$, $\tilde{\beta}_{II} = \omega\bar{n}_{II}/c - j\alpha_3/2$. $\bar{n}_I$ and $\bar{n}_{II}$ are the refractive indices of corrugation. The overall transfer matrix of the Bragg section consisting of M periods is obtained by

$$T_G = \prod_{i=1}^{M}[T] \qquad (13)$$

The effect of facet reflectivity is considered via multiplying T_G by appropriate matrix describes the facet reflectivity at the right end. The reflection of the DBR section is given by

$$r_{DBR} = \frac{T_{G21}}{T_{G11}} \qquad (14)$$

where T_{G21} and T_{G11} are the elements of the overall transfer matrix of DBR section.

C. Tuning Behaviour

The tuning behaviour is obtained by using the rate equation determining the carrier densities in the DBR sections along with appropriate relations describing the carrier induce index and absorption variations [6], [9], [16]. The carrier densities are related to the injection current densities by rate equations:

$$\frac{dN_1}{dt} = \frac{J_1}{ed_1} - N_1\left(\frac{1}{\tau_s} + B_1N_1 + C_1N_1^2\right) - v_g A_0(N_1 - N_0)(1-\varepsilon P)P \qquad (15)$$

$$\frac{dP}{dt} = v_g\Gamma_1 A_0(N_1 - N_0)(1-\varepsilon P)P - v_g(2\alpha'_{th} + \alpha_0)P \qquad (16)$$

$$\frac{dN_i}{dt} = \frac{J_i}{ed_i} - N_i\left(\frac{1}{\tau_s} + B_2N_i + C_2{N_i}^2\right), \quad i = 2,3 \qquad (17)$$

With J_1, J_2, J_3 are the current densities in the active, phase and grating sections, respectively. e is the electronic

charge, d_1 is the active layer thickness, v_g is the group velocity in the active section, A_0 is the gain/carrier density slope, N_0 is the transparency carrier density, ε is the gain compression factor, S is the photon density distribution in the active region, τ_s is the linear recombination time, B_1 and B_2 are the bimolecular recombination coefficient and C_1 and C_2 are the Auger recombination coefficient in the active and passive sections, respectively. P represents the uniform photon density along the active section. By considering the effect of injection current to the phase and grating sections, the oscillation condition becomes:

$$\Gamma_1 g_1 = (2\alpha'_{th} + \alpha_1) = \Gamma_1 A_0 (N_1 - N_0) \quad (18)$$

α'_{th} is threshold gain for a given injected current density J_2 or J_3. The photon density P inside the active region can be determined by (15) and (18). The features of numerical processing for tuning mechanism can be described as follows. The oscillation parameters $(\omega_{th}^m, \alpha_{th}^m)$ are calculated at threshold with zero injected current in all passive sections. By applying I_{PC} and I_{DBR}, refractive index and absorption coefficient of passive sections are modified and new oscillation condition is calculated. The photon density of main mode is altered by (15) and (18) and then new refractive index of active region is calculated. The new refractive index of refraction $\bar{n}_1$ is introduced in the model and the oscillation parameters are computed again, this procedure is repeated until a point of convergence is reached where the net threshold gains and lasing wavelengths change no more. Finally, the wavelength and output power of the main mode of oscillation are calculated. The flow-chart is shown in Fig. 2.

III. RESULTS AND DISCUSSION

We will present theoretical results showing the tuning characteristics of a three-section DBR laser. We illustrate the influence of a loss and/or reflection of energy at the active-passive interface on the tuning characteristics. The value of the material and structure parameters of laser used in this case is derived from [6], [9].

A. Tuning characteristics in ideal case
($C_L = 0$, $R = 0$, $R' = 0$)

Tuning characteristics of three-section DBR with no reflection or loss of energy at the active – passive interface are shown in Figs. 3-5. Fig. 3. shows wavelength tuning curves for dominant mode, Fig. 4 shows the output photon density variation of dominant mode during tuning process and Fig. 5 shows variation of threshold current. Mode jumps are apparent in all figures. The dashed curve in Fig. 3(a) shows the Bragg frequency shift. The characteristic sublinear behaviour is due to the saturation of the carrier density N_3 resulting from radiative and auger recombination.

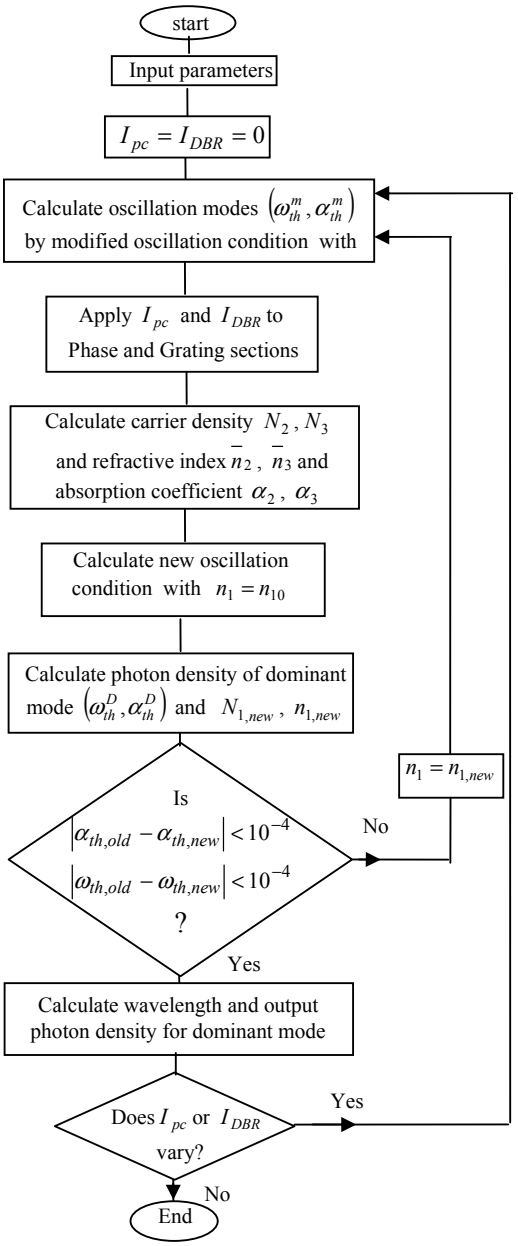

Fig. 2. Flow-chart for investigating tuning characteristics

B. Tuning characteristics in practical case
($C_L \neq 0$, $R \neq 0$ and $R' \neq 0$)

Figure (6) shows the effect of C_L on the tuning characteristics as a function of DBR and phase current. In this case the coupling of energy between the active and passive sections is given by $1 - |C_L|^2 - |S_{22}|^2$. Figure (7) shows the effect of reflection *(R=R')* on the dominant mode wavelength, discrete variation of wavelength is apparent (generation a new mode) where an alternation between two different modes

is observed. Main lobe of net threshold gain is shown in Fig. 8. The mode generation can be found by comparing Fig. 7 and Fig. 8.

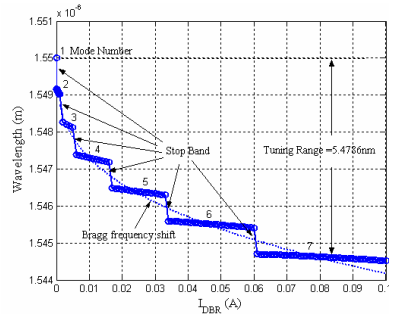

(a)

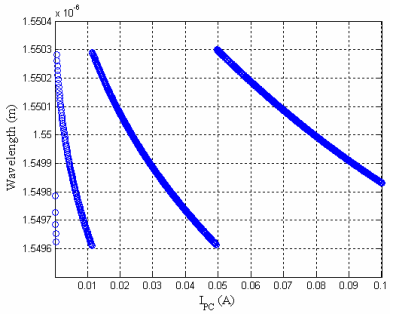

(b)

Fig. 3. Tuning curves for the dominant mode with $C_L = 0$, $R = 0$, $R' = 0$ as function of (a) DBR current, (b) Phase current

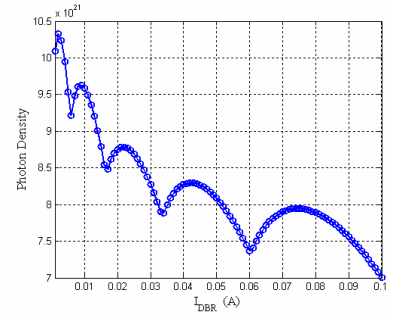

(a)

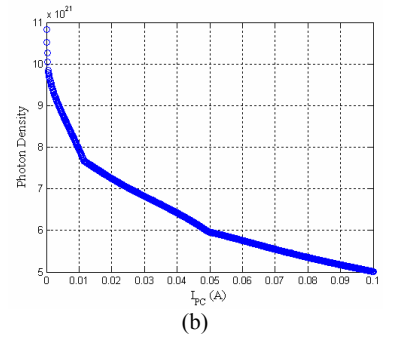

(b)

Fig. 4. Tuning curves for the output photon density with $C_L = 0$, $R = 0$, $R' = 0$ as function of (a) the DBR current (b) Phase current

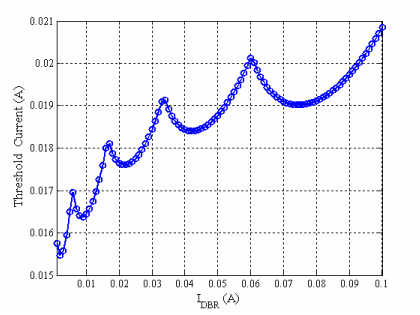

(a)

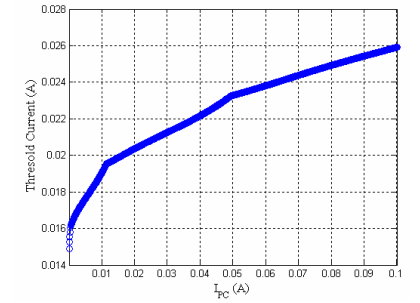

(b)

Fig. 5. Tuning characteristics of threshold current with ($C_L = 0$, $R = 0$, $R' = 0$) as a function of (a) DBR current (b) Phase current

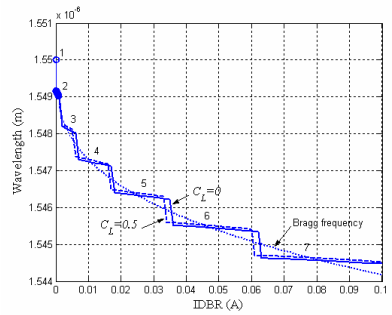

(a)

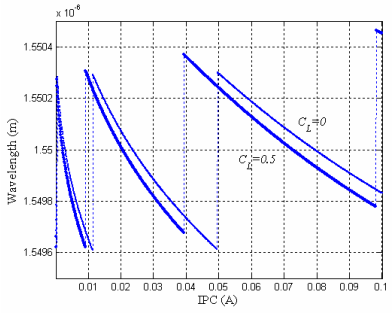

(b)

Fig. 6. Dominant mode wavelength variation as function of (a) DBR current (b) phase current *(R=R'=0)*

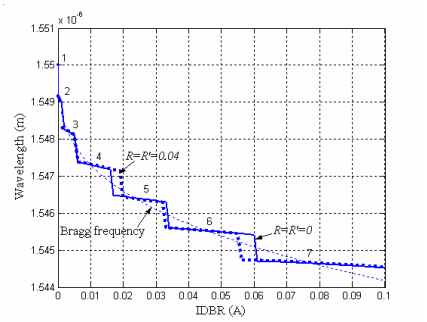

(a)

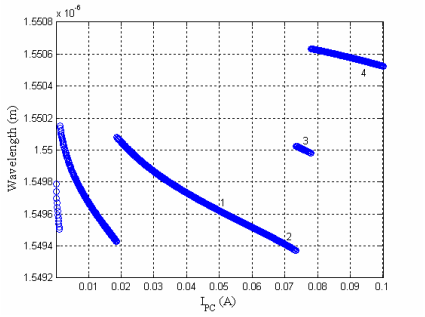

(b)

Fig. 7. Dominant mode wavelength variation as function of (a) DBR current (b) phase current *(C_L =0)*

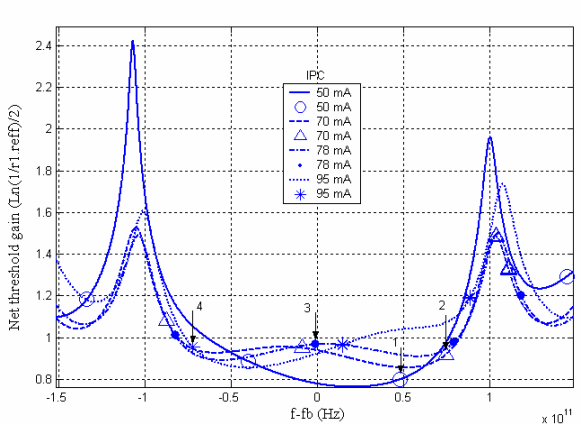

Fig. 8 Main lobe of net threshold gain (Numbers 1,2,3 and 4 are the same as the numbers showing on Fig. 7.)

IV. CONCLUSIONS

In this paper we have presented a rigorous model for three-section DBR laser with and without loss and reflection effects at active passive interface. By definition the effects of loss and reflection on oscillation condition equations the exact tuning characteristics are computed. Analysis shows that tuning characteristics of the three- section DBR are affected by the presence of reflections and/or loss of energy between active and passive sections. Loss at active - passive interface causes a shift in wavelength tuning characteristics. Reflection causes a generation of new mode in cavity and the range of continuous frequency shift is strongly dependent on the parameter R and R'.

REFRENCES

[1] L. A. Coldren, G. A. Fish, Y. Akulova, J. S. Barton, L. Johansson and C. W. Coldren, "Tunable Semiconductor Lasers: A Tutorial," *IEEE J. Lightwave Technol*., vol. 22, pp. 193-202, 2004.

[2] L. A. Coldren, "Monolithic Tunable Diode Lasers," *J. on Selected Topics in Quantom Electron*., vol. 6, pp. 988-999, 2000.

[3] E. Bruce, "Tunable Lasers," *IEEE Spectrum*, February, 2002.

[4] T. L. Koch and U. Koren, "Semiconductor Lasers for Coherent Optical Fiber Communications," *IEEE J. Lightwave Technol.*, vol. 8, pp. 274-293, 1990.

[5] K. Komori, S. Arai, Y. Suematsu, I. Arima and M. Aoki. "Single-Mode Properties of Distributed-Reflector Lasers," *IEEE J. Quantom Electron.,* vol. 25, pp. 12351244, 1989.

[6] X. Pan, H. Olesen and B. Tromborg " A Theoretical Model of Multielectrode DBR Lasers," *IEEE J. Quantum Electron.,* Vol. 24, pp. 2423-2432, 1988

[7] E. Patzak, P. Meissner and D. Yevick, "An Analysis of the Linewidth and Spectral Behavior of DBR Lasers," *IEEE J. Quantum Electron.,* vol. QE-21, No. 9, pp. 1318-1325, 1985.

[8] N. P. Caponio, M. Goano, I. Maio, M. Meliga, G. P. Bava, G.D. Anis and I. Montrosset "Analysis and Design Criteria of Three-Section DBR Tunable Lasers," *IEEE J. on Selected Areas in Commun.,* vol 8, pp.1203-1213, 1990.

[9] A. Tsgopoulos, T. Sphicopoulos, I. Orfanos and S. Pantelis "Wavelength Tuning Analysis and Spectral Characteristics of Three-Section DBR Lasers," *IEEE J. Quantum Electron.,* vol. 28, pp. 415-426, 1992

[10] L. G. Kazovsky, M. Stern, S. G. Menocal and C. Zah, " DBR Active Optical Filters: Transfer Function and Noise Characteristics," *IEEE J. Lightwave Technol.,* vol. 8, pp.1441-1450, 1990.

[11] M. Teshima, " Dynamic Wavelength Tuning Characteristics of the 1.5-μm Three-Section DBR Lasers: Analysis and Experiment," *J. Quantum Electron.,* vol.31, pp. 1389-1400 , 1995.

[12] G. Bjork and O. Nilsson, "A New Exact and Efficient Numerical Matrix Theory of Complicated Laser Structures; Properties of Asymmetric Phase-Shifted DFB Lasers," *J. Lightwave Technol.,* vol. LT-5, pp. 140-146, 1987.

[13] J. Hong, W. Huang and T. Makino, "On the Transfer Matrix Method for Distributed-Feedback Waveguide Devices," *J. Lightwave Technol*., vol.10, pp.1860-1868, December, 1992.

[14] I. Orafanos, T. Sphicopoulos, A. Tsigopoulos, C. Caroubalos, "A Tractable Above-Threshold Model for the Design of DFB and Phase-Shifted DFB Lasers," *IEEE J. Quantum Electron.,* vol. 27, pp. 946-956, 1991.

[15] L. A. Coldren and S.W Corzine, Diode Lasers and Photonic Integrated Circuits. John wiley and Sons, California, 1995.

[16] M. G. Davis and R. F. O'Dowd, "A New Large-Signal Dynamic Model for Multielectrode DFB Lasers Based on the Transfer Matrix Method," *IEEE Photonic Tecnol. Lett.,* vol. 4, pp. 838-840 , 1992

[16] M. C. Amann and J. Buss, Tunable Laser Diodes. London, Artech House, 1998.

[17] B. Tromborg, H. Olesen, X. Pan, and S. Satio " Transmision Line Description of Optical Feedback and Injection Locking for Fabry-Perot and DFB Lasers," *IEEE J. Quantum Electron.,* vol. QE-23, pp. 1875-1889, 1987.